

## Conductive mesh based flexible dye-sensitized solar cells

Xing Fan, Fuzhi Wang, Zengze Chu, Lin Chen, Chao Zhang, and Dechun Zou<sup>a)</sup>

Beijing National Laboratory for Molecular Sciences, Key Laboratory of Polymer Chemistry and Physics of Ministry of Education, College of Chemistry and Molecular Engineering, Peking University, Beijing 100871, China

(Received 8 October 2006; accepted 15 January 2007; published online 12 February 2007)

Conductive meshes are used to replace transparent conducting oxides (TCOs), which are commonly used in electrodes of dye-sensitized solar cells (DSSCs). The TCO-less flexible working electrode could be sintered under 400–500 °C. A preliminary result that open-circuit voltage ( $V_{OC}$ ) = 650 mV, short-circuit current density ( $I_{SC}$ ) = 4.5 mA/cm<sup>2</sup>, and efficiency ( $\eta_{AM1.5}$ ) = 1.49% (100 mW/cm<sup>2</sup>) is obtained from the liquid-type DSSC. The incident light could be dispersed uniformly inside the electrode. Testing results of the double-counterelectrode cell indicate that the transmission of electrolyte is not the rate-determining step. The dense TiO<sub>2</sub> layer is critical in improving the cell's performances. © 2007 American Institute of Physics.

[DOI: 10.1063/1.2475623]

Dye-sensitized solar cells (DSSCs) are being rapidly developed as the next generation of photovoltaic cells following Si-based solar cells.<sup>1–9</sup> In view of DSSCs' high efficiency, cheap price, environmental friendliness, low angle dependency on incident light, and many other advantages, they have gained more and more attentions from both the academe and industry. At present, the  $\eta_{AM1.5}$  of a transparent conducting oxide (TCO) glass-based liquid-type DSSC has exceeded 11%,<sup>10,11</sup> 8.2%,<sup>12</sup> and 6% (Ref. 13) for a small-area (~0.2 cm<sup>2</sup>) cell, large-area strip-shaped cell (5 × 0.8 cm<sup>2</sup>), and large-area module (a single cell's area is 18 × 0.8 cm<sup>2</sup>), respectively. However, during the DSSC's application process, flexibility has become a challenge. Flexible DSSCs are not only convenient for transportation but also more beneficial when used in more complex environments. The key to a flexible DSSC is to produce a flexible working electrode, which requires that the substrate should own high conductivity, transparency, and high temperature sinterability besides flexibility. However, not many flexible substrates are available for choices. At present, they mainly use poly(ethylene terephthalate (PET)/indium tin oxide (ITO) as the substrate.<sup>14–17</sup> Miyasaka and Kijitori used PET/ITO/TiO<sub>2</sub> as the working electrode and rigid platinized fluorine-doped tin oxide glass as the counterelectrode, and the small-area (0.2 cm<sup>2</sup>) liquid-type DSSC's  $\eta_{AM1.5}$  reached 4.1% (100 mW/cm<sup>2</sup>).<sup>18</sup> Meanwhile, Lindstrom *et al.* used PET/ITO as the substrate of the working electrode, and the all-plastic DSSC's  $\eta_{AM1.5}$  was still lower than 2.3% (100 mW/cm<sup>2</sup>).<sup>19,20</sup> One difficulty in using a PET/ITO substrate is the heat resistance limit, and this makes the TiO<sub>2</sub> electrode generally sinterable only under 200 °C, which is not the optimum sintering temperature, i.e., 400–500 °C. Moreover, it is very difficult to produce the PET/ITO substrate with high transparency and good conductivity. Hence, conductivity is the only important factor that constrains the improvement of flexible DSSC performance, especially with an increase in cell area. In relation to this, Kang *et al.*<sup>21</sup> reported a flexible DSSC (effective area is 0.2 cm<sup>2</sup>) assembled with flexible stainless steel sheet as the substrate

and its  $\eta_{AM1.5}$  reached 4.2% (100 mW/cm<sup>2</sup>). However, they had to use Pt-coated PET/ITO as the counterelectrode due to the opacity of the working electrodes.

In short, DSSCs at present have still not rid of their dependence on TCOs. TCOs' resistance factor is higher than that of metallic materials by two to three orders of magnitude, and its production cost is quite high. For a polymer/TCO substrate, it is prone to stripping and damaged electrode surfaces due to stress fatigue. In order to address these problems, especially flexible DSSCs' heat resistance, conductivity, long-term light/heat stability, mechanical strength, bending endurance, and cost, further experiments need to be carried out on DSSCs' electrode structure.

This letter reports a type of DSSC working electrode structure. A TCO-less conductive and flexible mesh is introduced into DSSC's working electrode, which makes it possible for the working electrode to be sintered under high temperature.

Working electrodes were fabricated according to the patent,<sup>22</sup> and the TiO<sub>2</sub> colloid was produced according to the second method in the literature.<sup>2</sup> The dense TiO<sub>2</sub> layer (DTL) solution used was the ethanol solution of titanium isopropoxide (ACORS) (0.01M)/acetyl acetone (0.02M). The stainless steel mesh was cleaned and degreased in acetone and then was presintered at 500 °C for 15 min. Then the mesh was dipped in the DTL solution for 30 s, taken out, and then sintered at 500 °C for 15 min; this process was repeated thrice. The diluted TiO<sub>2</sub> colloid was homogeneously sprayed on both sides of the mesh while being baked under the illumination of an infrared lamp, and then it was sintered at 500 °C for 30 min. The thickness of the porous TiO<sub>2</sub> layer (PTL) was controlled by the TiO<sub>2</sub> colloid's concentration and spray time. Finally, the sintered TiO<sub>2</sub> electrode was cooled to about 100 °C, dipped into 3 × 10<sup>-4</sup> M N3 dye [*cis*-bis(isothiocyanato) bis(2,2'-bipyridyl)-4,4'-dicarboxylato)-ruthenium(II)], and maintained for 12 h. The electrode was treated with 4-*tert*-butylpyridine (Aldrich) according to the method in the literature<sup>5</sup> before testing.

The electrode's morphology was observed via scanning electron microscope (SEM) (S570 Hitachi). The counterelectrode was a 0.05 mm thick Pt foil (purity: 99.9%); the electrolyte was mixed with a solvent that contained 0.5M LiI

<sup>a)</sup>FAX: +86-10-62759799; electronic mail: dczhou@pku.edu.cn

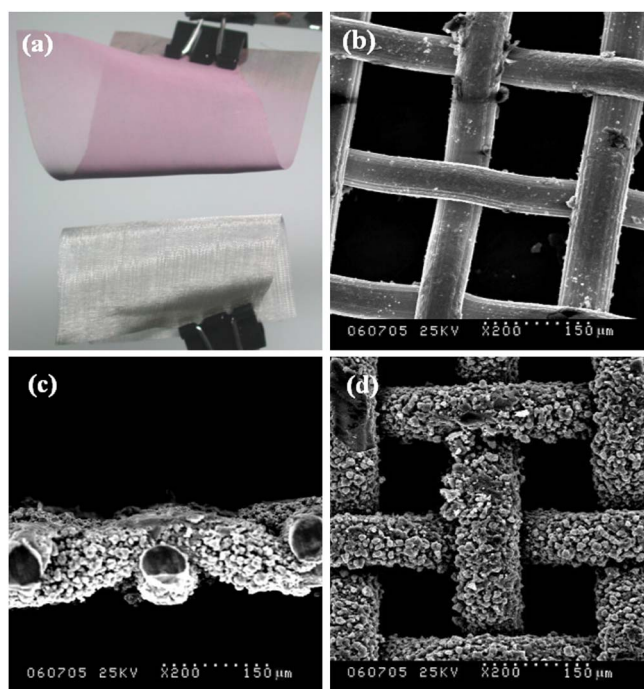


FIG. 1. (Color online) (a) Optical photo of the as-prepared electrode (upper,  $4.5 \times 7 \text{ cm}^2$ ) and the net substrate (lower,  $4 \times 5.5 \text{ cm}^2$ ); (b) SEM photos of the mesh substrate; [(c) and (d)] top and sectional views of the as-prepared electrode.

(Aldrich) and  $0.05M \text{ I}_2$  (AR) 3-methyl-2-oxazolidinone (Aldrich)/ $\text{CH}_3\text{CN}$  (1:9). The working electrode, electrolyte, and counterelectrode were assembled into a sandwich structure. The cell's active area was  $0.33 \text{ cm}^2$ , the simulated solar light source was YSS-50A (Yamashita DESO), and the light intensity was  $100 \text{ mW/cm}^2$ .

Figure 1(a) shows a large-area ( $45 \times 70 \text{ mm}^2$ ) flexible working electrode, from which it can be seen that this kind of electrode has relatively good flexibility since the interlaced metal wires could have slight relative displacement between them when the mesh is subjected to external force. The mesh substrate has less strain and stress concentration at the substrate/ $\text{TiO}_2$  interface than PET/ITO or a stainless steel sheet substrate, thus enhancing the bending fatigue resistance of the electrode. Figure 1(b) is a SEM photo of the metallic mesh before coating. It has 120 meshes and the diameter of the metal wire is about  $0.067 \text{ mm}$ ; the mesh thickness is about  $0.150 \text{ mm}$ , and the square mesh's width is also about twice the wire's diameter. Figures 1(c) and 1(d) are the SEM photos of the sectional view and the top view of the sensitized working electrodes, from which it could be seen that the PTL wraps closely at the surface of the interlaced metal wires. The experimental results indicate that the conductivity and mechanical strength of the mesh were not influenced much even when sintered at  $500^\circ\text{C}$ . A flexible  $\text{TiO}_2$  electrode could be produced with fewer restrictions. This brings much convenience to large-area and large-scale production. Figures 1(c) and 1(d) also show that the meshes were not totally closed after coating the PTL; the size of the remaining meshes was decided by both the number of meshes and the thickness of the PTL. Preliminary experimental results indicate that the existence of meshes is quite important. These meshes provided sufficient passage for both light and electrolyte. Moreover, the mesh electrode's nonflat structure and the PTL could jointly provide enough reflection

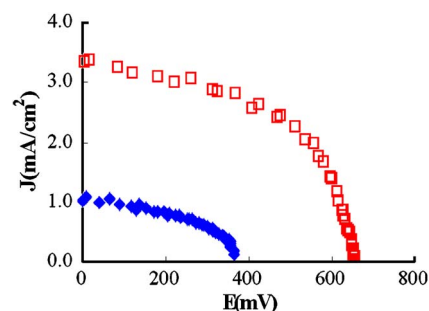


FIG. 2. (Color online)  $I$ - $V$  performance of the electrode with (□) or without (◆) DTL based on the 120 mesh net substrate and an  $8 \mu\text{m}$  thick PTL-AM1.5,  $100 \text{ mW/cm}^2$ .

and diffusion centers. The incident light will not leave the electrode simply through specular reflection or direct penetration. It can be dispersed through the entire working electrode in a zigzag or more complex manner. The photon capture rate of the working electrode will then be improved, and the light angle dependency can be further reduced. This is an active factor in improving the average light-electricity conversion efficiency during a day.

Figure 2 shows the working curves of a DSSC based on this kind of flexible working electrode, where ◆ represents the case without a DTL and □ represents the case with a DTL. Figure 2 shows that, after inserting the DTL, both  $I_{\text{SC}}$  and  $V_{\text{OC}}$  apparently increased.  $V_{\text{OC}}$  especially reached about  $650$  or even  $700 \text{ mV}$  at the highest. The experimental results also indicate that cell stability after the insertion of DTL apparently improved, which proves that DTL could effectively inhibit the back transfer of electrons and also protect the metal substrate from the corrosion of the electrolyte. The optimization of the DTL and the reduction of leak points in electrodes are important in further studies on improving a DSSC's overall conversion efficiency due to the specialty of this kind of mesh structure.

Figure 3 represents the PTL thickness dependence of the cell performance (all 120 meshes). It could be observed that both  $V_{\text{OC}}$  and  $I_{\text{SC}}$  show an increasing pattern followed by a decreasing one when PTL becomes thicker. When PTL is  $10 \mu\text{m}$  thick, the cell's  $I_{\text{SC}}$ ,  $V_{\text{OC}}$ , and  $\eta_{\text{AM1.5}}$  reach  $4.5 \text{ mA/cm}^2$ ,  $650 \text{ mV}$ , and  $1.49\%$ , respectively. This trend can be explained as follows. When PTL is too thin, light scattering due to the PTL is too weak, the electrode's shadow side is in a poor working state, and the overall working voltage is low. Moreover, the insufficient absorbance of dye will also cause low current. When PTL is too thick, the transmission process of the electrolyte inside the  $\text{TiO}_2$  layer's micro-

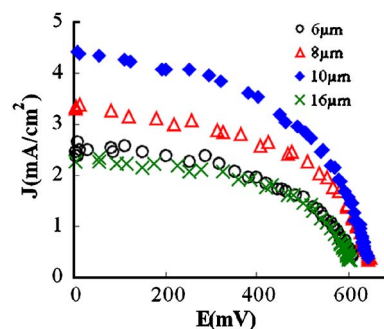


FIG. 3. (Color online)  $I$ - $V$  performance of the electrode with different thicknesses of  $\text{TiO}_2$ . AM1.5,  $100 \text{ mW/cm}^2$ .

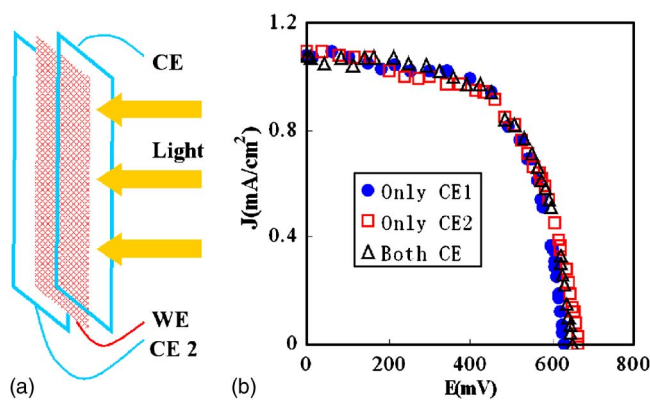


FIG. 4. (Color online) (a) Structure of DCEC; (b)  $I$ - $V$  performance of DCEC with only CE1 (●); only CE2 (□); both CEs (□).

hole is restricted, which causes the serious interface polarization of electrodes and reduces cell performance.

To study the illumination site and transmission of carriers at each side of the mesh electrode, we designed a double-counter electrode cell (DCEC) device in which two counter-electrodes share one working electrode, as shown in Fig. 4(a). Evidently, this cell structure could not be realized by a traditional DSSC working electrode. Both counterelectrodes (CE1 and CE2) were ITO glass sputtered with 4 nm Pt. We compared the cell's  $I$ - $V$  characteristics when only CE1 or CE2 was connected and both CE1 and CE2 were connected into the working circuit. The experimental results are shown in Fig. 4(b). Although the cell is only illuminated at one side, three curves almost have the same shape. This result explains two important issues. First, as discussions for Fig. 1 stated, thanks to the PTL and mesh structures, the light inside the electrode was well dispersed, and the total illumination conditions at each side are basically the same. Second, although the electrode's apparent thickness increased, the entire cell's rate-determining step is not the transmission process of the oxide species in the electrolyte. The electrode at the shadow side can effectively reduce oxide species produced at both sides. The results above also indicate that the entire PTL coated around the metal wire could be regarded as active area; the area loss due to the opaque mesh part can almost be compensated. Since the working electrode itself is transparent, the electrode's substrate material would not have to be transparent, which means that this type of DSSC could completely get rid of its dependency on TCOs.

We came up with a type of meshlike DSSC flexible working electrode and produced DSSCs without any TCO. As compared to polymer/ITO or the stainless steel sheet substrate, this working electrode has good conductivity, high heat resistance, and better long-term heat stability besides its good transparency, which brings greater freedom for the fabrication of a working electrode and the choice of counter-

electrode. The experiments prove that the DTL is critical in improving this flexible DSSC's performance. Moreover, the DCEC experiments indicate that the entire cell's rate-determining step is not the transmission process of oxide species in electrolyte. Thanks to the strong light scattering capability of the mesh and the PTL, the light inside the electrode could be distributed homogeneously at both sides. Finally, we think that the optimization of the DTL will be important on further improvement of this kind of flexible DSSC in the future.

This research was supported by NSF and 973 programs of the People's Republic of China, under Grant Nos. 90401028, 50673003, and 2002CB613405.

- <sup>1</sup>B. O'Regan and M. Graetzel, *Nature (London)* **353**, 737 (1991).
- <sup>2</sup>A. Kay, M. K. Nazeeruddin, I. Rodicio, R. Humphry-Baker, E. Müller, P. Liska, N. Vlachopoulos, and M. Grätzel, *J. Am. Chem. Soc.* **115**, 6382 (1993).
- <sup>3</sup>M. Durr, A. Bamedi, A. Yasuda, and G. Nelles, *Appl. Phys. Lett.* **84**, 3397 (2004).
- <sup>4</sup>J. B. Baxter and E. S. Aydil, *Appl. Phys. Lett.* **86**, 053114 (2005).
- <sup>5</sup>H. X. Wang, H. Li, B. F. Xue, Z. X. Wang, Q. B. Meng, and L. Q. Chen, *J. Am. Chem. Soc.* **127**, 6394 (2005).
- <sup>6</sup>P. Wang, C. Klein, R. Humphry-Baker, S. M. Zakeeruddin, and M. Grätzel, *Appl. Phys. Lett.* **86**, 123508 (2005).
- <sup>7</sup>Y. Chiba, A. Islam, R. Komiya, N. Koide, and L. Y. Han, *Appl. Phys. Lett.* **88**, 223505 (2006).
- <sup>8</sup>S. Ito, S. M. Zakeeruddin, R. Humphry-Baker, P. Liska, R. Charvet, P. Comte, M. K. Nazeeruddin, P. Pechy, M. Takata, H. Miura, S. Uchida, and M. Grätzel, *Adv. Mater. (Weinheim, Ger.)* **18**, 1202 (2006).
- <sup>9</sup>P. R. Somani, S. P. Somani, M. Umeno, and A. Sato, *Appl. Phys. Lett.* **89**, 083501 (2006).
- <sup>10</sup>F. D. Angelis, M. K. Nazeeruddin, S. Fantacci, A. Selloni, G. Viscardi, P. Liska, S. Ito, B. Takeru, and M. Graetzel, *J. Am. Chem. Soc.* **127**, 16835 (2005).
- <sup>11</sup>A. Islam, Y. Chiba, Y. Watanabe, R. Komiya, N. Koide, and L. Han, *Jpn. J. Appl. Phys., Part 2* **45**, L638 (2006).
- <sup>12</sup>M. Spath, P. M. Sommeling, J. A. M. van Roosmalen, H. J. P. Smit, N. P. G. van der Burg, D. R. Mahieu, N. J. Bakker, and J. M. Kroon, *Prog. Photovoltaics* **11**, 207 (2003).
- <sup>13</sup>S. Y. Dai, K. J. Wang, J. Weng, Y. F. Sui, Y. Huang, S. F. Xiao, S. H. Chen, L. H. Hu, F. T. Kong, X. Pan, C. W. Shi, and L. Guo, *Sol. Energy Mater. Sol. Cells* **85**, 447 (2005).
- <sup>14</sup>M. Tomiha, S. Uchida, H. Takizawa, and M. Kawaraya, *Sol. Energy Mater. Sol. Cells* **81**, 135 (2004).
- <sup>15</sup>M. Tomiha, S. Uchida, N. Masaki, A. Miyazawa, and H. Takizawa, *J. Photochem. Photobiol., A* **164**, 93 (2004).
- <sup>16</sup>M. Durr, A. Schmid, M. Obermaier, S. Rosselli, A. Yasuda, and G. Nelles, *Nat. Mater.* **4**, 607 (2005).
- <sup>17</sup>D. S. Zhang, T. Yoshida, T. Oekermann, K. Furuta, and H. Minoura, *Adv. Funct. Mater.* **16**, 1228 (2006).
- <sup>18</sup>T. Miyasaka and Y. Kijitori, *J. Electrochem. Soc.* **151**, A1767 (2004).
- <sup>19</sup>H. Lindstrom, A. Holmberg, E. Magnusson, S. E. Lindqvist, L. Malmqvist, and A. Hagfeldt, *Nano Lett.* **1**, 97 (2001).
- <sup>20</sup>H. Lindstrom, A. Holmberg, E. Magnusson, L. Malmqvist, and A. Hagfeldt, *J. Photochem. Photobiol., A* **145**, 107 (2001).
- <sup>21</sup>M. G. Kang, N. G. Park, K. S. Ryu, S. H. Chang, and K. J. Kim, *Sol. Energy Mater. Sol. Cells* **90**, 574 (2006).
- <sup>22</sup>Xing Fan, Dechun Zou, and Rong Jian, China Patent No. 200610089645.2 (Oct. 8, 2006).